

High vacuum phase transformation of fluorspar vapors to crystal aggregates

J. Mouhovski*, O. Vitov, V. Dimov, B. Kostova, S. Gechev

*Institute of Mineralogy and Crystallography "Acad. Ivan Kostov",
Bulgarian Academy of Sciences, Acad. Georgy Bonchev Str., bl.107, 1113 Sofia, Bulgaria*

Received April 4, 2013; Accepted April 24, 2013

Complex crystal aggregates from fluorspar are grown from vapor phase at specific P - T conditions. Quasi-equilibrium for occurring mass-transport processes, phase transformations and crystal-chemical reactions is attained in multicameral mode crucible by changing the temperature pressure imposed on molten portions of the used natural fluorite and/or by varying the gas-permeability of the channels connecting different sections in crucible interior to vacuum ambient. The sizes of the channels are reduced to provide Knudsen type diffusion thus limiting the induced vapor fluxes through them leading to super-saturation inside the peripheral crucible compartment. The grown aggregates reveal a complicated habit formed during three stages growing process provided by relevant thermodynamic and phases. The residual stresses in the aggregates are not observed whereas those in simultaneously grown boules from the non-vaporized melts in crucible cameras are clearly distinguished. The optical transmittance of the boules are considerably higher, especially in the UV, comparing to that of crystal aggregates, showing several peaks of specific light-absorption due to enhanced presence of rare-earth (RE) impurities. The aggregates manifest their nearly full reflectivity from visible to near IR region. The growth mechanisms from vapor phase by using natural fluorite with RE are explained on thermodynamic grounds that allows the processes being put under reliable control. The results are anticipated to help for developing new perspective techniques for vapor phase growth of several fluoride compounds with complex structure and composition but with wide application. Similar growth mechanisms for CaF_2 crystals are speculated being possible on the Moon in its very early period of formation.

Keywords: crystal structure, mass transfer, phase equilibrium, purification, optical medium

INTRODUCTION

The growth mechanism of calcium fluoride – as product of ore mineralization or artificially grown crystals – depends on thermodynamic and crystal-chemical conditions of the surrounding medium. Both the crystal habit and crystallographic character of crystal faces can be changed in accordance with P - T mineralization conditions and solutions chemistry. It was firmly established crystal transition from octahedral to cubic form via some more complex intermediate forms [1]. The habit of the real crystals is, as a rule, not geometrically regular that is due to irregularity in the mass-transport for supplying substance. One-directional supply has been proved to distort gradually the cubic crystal to mosaic block, rod-like or lamellar whereat the symmetry decreases, the habit becoming in some cases completely irregular.

The exact reconstruction of the existed thermodynamic and crystal-chemical conditions during the growth of CaF_2 natural or artificial crystals appears a challenging task since it helps the researchers to clarify the variety of interrelating factors that may influence considerably the crystal

alterations during ore mineralization as well as during the application of the already developed growing techniques (from solution, melt or vapor). In the present paper the accent is put on the growth of CaF_2 crystals from vapor phase as the less explored technique as compared to growth from solution and especially to growth from melt [2].

The object in study – single CaF_2 – has been won recognition as preferable in many cases optical medium for manufacturing optical elements appropriate to satisfy the fast increasing needs of large scale optics in deep ultra violet (UV), visible (Vis) and infrared (IR) spectral regions. Since the direct usage of natural fluoride for manufacturing thereof optical elements is strongly restricted due to impossibility, in practical, to be found sufficiently homogeneous large single crystals with minimum structural defect, the fluorspar has to be transformed appropriately to sintered or polycrystalline precursors that to be used as starting material. On this ground several industrial techniques have been developed for growing an artificial fluorite from melt [2] unlike the growth of CaF_2 crystals in over-saturated solutions where the small sizes, incomparably lower crystallization rate,

* To whom all correspondence should be sent:
E-mail: jmouhovski@abv.bg

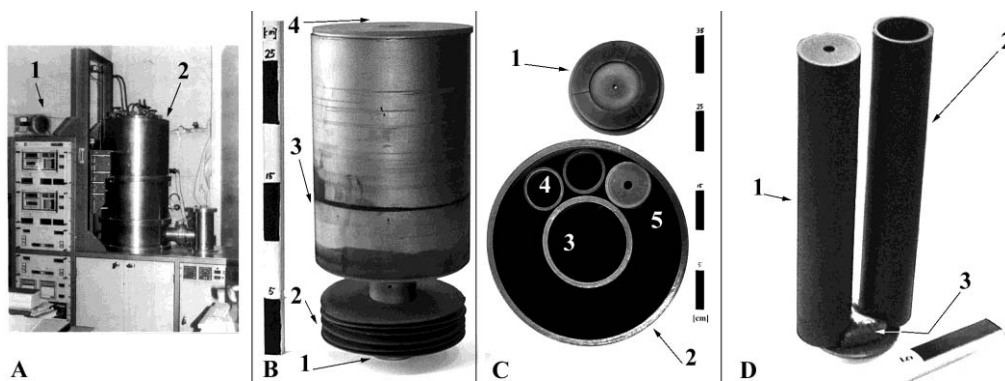


Fig. 1. A – Apparatus for crystal growing by BS method with furnace control panel assy (1) and growing chamber (2); B – multicameral graphite crucible with supporting tail-end (1), batch of separated heat-adjusting Mo-rings (2), cylindric body (3) and general cover with axially drilled channel (4); C – cross-section of multicameral crucible with a central camera (3) and up to 9 peripheral inserts (4), covered with corresponding lids (1) and (5). Some of the lids can be taken away to accelerate the melt vaporization; D – view of two peripheral inserts (1) and (2), in-between the bottom section of which a fluorospar condensate is formed by a shape of segment (3).

and uncontrollable arising lattice defects have made it groundless. Nevertheless the latest very strict requirements of vacuum UV and UV-laser optics put higher challenges before the growers as concerning the purity of starting fluorospar and final product and the cost of the later. Here the Single Crystal Technology appears a promising method for increasing significantly the yield of high-sized CaF_2 crystals [3].

Without comparable industrial effect but submitting several specific scientific issues appeared the growth of CaF_2 crystals from fluorospar vapor containing some REs impurities. Such starting material was used for development of original Bridgman-Stockberger (BS) growing technique where, in multi-camera crucible with original construction, several boules were grown from melts while inhomogeneous substance was crystallized from vapor phase in supersaturated peripheral crucible compartment [4]. At that the RE content in the grown boules can be substantially reduces at the expense of enriched correspondingly to RE vapor grown substance. The technique's efficiency depends on the ability a given RE to form a stable fluoride composition, the ionized molecules of which may evaporate easily at the temperature of the molten starting fluorospar and the pressure over its surface. It was approved the process can be put under control if an appropriate P - T equilibrium was kept in all crucible cameras. These cameras represent several inner axial-symmetric inserts, loaded with starting grained purified fluorospar (or thereof made precursors), and put in a *peripheral compartment* (PC) with annular cross-section (Fig. 1B, C). A central compartment – “crucible core” – was also loaded with another

portion of fluorospar. One may adjust P - T conditions inside the crucible so that to provide an intensive bulk boiling in all peripheral and central melts. This way vaporized material supersaturated the free space in the PC, initiating nucleation upon its coolest bottom section to start, during the slow crucible withdrawal towards the lower (“cold”) furnace zone. Thus formed crystallite was being enriched to those REs, the fluorides of which possessed sufficiently high vapor pressure to endure effective liquid to vapor phase transformation. As a resulting production represented a relatively cheap batch of parallel boules with very high and close to each other optical characteristics that may satisfy even the contemporary, mostly strict demands of VUV- and UV-optics whereas the PC sublimate, depending on the degree of its RE's concentration, can be used for manufacturing selective light-shutters.

The present survey aims at experimental and theoretical investigation of the possible phase transformations of fluorospar vapor in the above described multi-camera crucible at large varying P - T conditions, wherein the grown crystallite would be expected to possess unique structure and properties. This suggests to be determined the triple point (t.p.) phase diagram for the used fluorospar that would allow being studied the relevant alterations in quasi-equilibrium for the proceeding mass-transport phenomena and related kinetic reactions. The longitudinal cross section view of the grown crystallite would reveal how manner the crystal habit may change according to phase transformations mode. The results are anticipated to clarify the mechanisms and regularities that govern the processes and phenomena proceeding. This may

increase the significance of growing single and mixed crystal fluoride compounds from vapor phase by modification and/or optimization of the applied technique on the base on reliable thermodynamic grounds. From geological point of view the results can promote model simulations of some mineral-genetic processes grounded on HV low-gravity emissions that could be thought being existed on the Moon or other small sized space objects where similar conditions could whenever being existed.

MATERIAL, METHODS AND APPARATUS

The starting material – grained fluorospar – contained several tens ppm in total RE elements where cerium was the prevalent one [5].

The growing experiments were performed using BS apparatus (**Fig. 1a**), the furnace unit of which allows a precise control over the thermal field configuration.

Conditions for condensation or sublimation of fluorite vapors were created by super-saturating the free space in the PC of the above described multi-camera mode crucible made by low porous, high purity graphite. The crucible cameras were loaded by weighed out portions of fluorospar, mixed carefully with 2.4 wt.% PbF_2 that acted as scavenger during the heating stage, thus providing a removal – by chemical reactions – of the mostly oxygen-containing contaminants [6]. The free spaces in crucible cameras were connected to PC free space by parallel system of channels, drilled axially in corresponding cameras' lids. The gas-permeability of the channels, depending on their diameter and length, can determine as prevalent one of the three possible mass-transport mechanisms: Knudsen diffusion, normal diffusion or viscous flow. An axial channel in the outer cover of the crucible connected its interior to the vacuum chamber ambient. The partial and/or total effective gas-conductivities of such designed system of channels determine the established pressures inside the cameras and the PC at a given T -head imposed on the loaded crucible. The methodology consisted in providing an intensive vaporization of different in mass%, but significant partitions from the molten portions in the cameras at controlled P - T conditions, which led to super-saturation by fluorospar vapors of the free space inside the PC, with following therein crystallization of condensed and/or sublimated substance on the cooler surface of the flat bottom in-between the inserts, during the slow crucible withdrawal towards the cold furnace zone. Essentially, the experiments were

implemented as combined simultaneous crystal growing from melt (inside the cameras) and from vapor – in the PC.

The vaporized quantities were calculated as the differences between the initial and final gross weights in the loaded inserts. An average time-duration of the process was taken to estimate the vapor fluxes throughout the lids' channels.

The T -head upon the molten portions was altered to vary differently: up to 34 K (“low” head), from 35 to 160 K – “intermediate” head and above 160 K – “high” head. This way a sequence of physical-chemical and/or crystal-chemical processes was initiated leading to shift in desorption/adsorption equilibrium, evaporation/vaporization by melt boiling, condensation, ionic replacements into fluorite lattice, melt and vapor crystallization (sublimation).

Longitudinally processed probes of the crystallized material were investigated by optical microscope in reflected and transmitted light, electron microscope and electron-transmission microscope. The used transmission electron microscope (TEM) Phillips EM 420 worked with accelerating voltage of 100 kV. The needed specimens were prepared by the method of wet suspending after grinding in alcohol and deposition on a perforated carbon film with a thickness below 0.5 nm, mounted onto 3 mm diameter copper grid disks.

The spectral distribution of the optical transmission t was measured at room temperature on 2.0 ± 0.15 mm-thick bi-side polished parallel plates within an accuracy of ± 0.3 nm in the spectral range 195 – 800 nm using a Varian's UV-VIS spectrophotometer Cary 100. The absorption coefficient, α , was calculated via Beer-Lamber's formula $\alpha = d^{-1} \ln (1/t)$ with d being the sample thickness. These samples were tested as well for internal stresses in polariscope/polarimeter PKS-250 U.4.1.

The total internal reflection of fine grinding probes was measured by using Evolution 300 UV-VIS Spectrometer of THERMA.

RESULTS AND DISCUSSION

The condensation/sublimation of fluorite vapors was found to start on segmental areas between the particular inserts (**Fig. 1D and Fig. 2a**). At larger resolution it is seen each one segment was built up forming a basis representing pseudo-grained fluorite aggregate consisting in skeleton CaF_2 small crystals whereupon one may think being condensed and crystallized fluorite drops (**Fig. 2b**).

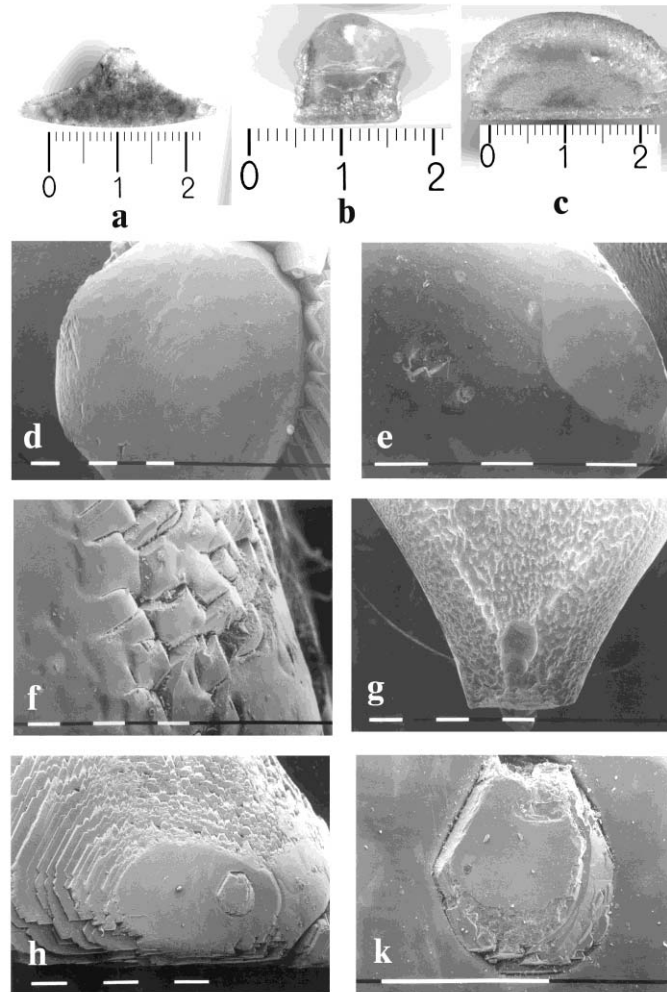


Fig. 2. Optical microscope pictures of crystallized material in the PC of multicameral crucible imposed 7 hours in HV at constant T -head, followed by 28 hours lasting crucible withdrawal with speed of 4 mm per hour in optimized furnace unit of BS apparatus. **a** – condensed fluorospar vapors with segmental shape; **b** - condensed and crystallized fluorite drops; **c** – selectively grown plate-like and acicular fluorite crystals; **d** – fluorite drops, surrounded by deeper globules, connected by fine particles of graphite and fluorite; **e, f** – different faceting of crystal faces for the condensed drops; **g** – equal in sizes pits on places found close to inserts' external surface; **h** – a stem-like single crystal with hexagonal cross-section, incorporated into a fluorite drop; **k** – scale up fragment of picture h.

On the surface of thus formed basis, numbers of plate-like and acicular crystals were grown selectively (**Fig. 2c**).

The basis with height of ≈ 4 mm was shown in **Fig. 2d** being built in light corns, surrounded by deeper globules with diameter of ≈ 1 mm connected by fine particles of graphite and fluorite. The drops, sized between 4 and 10 mm, turned out clear, without any inclusions and defects. The smaller ones were found close to ideal sphere while the bigger ones represented oblate spheroids. The basic-drops boundary was sharply manifested as the wetting angle between the sharp surface basic and the drops varied from 20 to 60 degrees of circle (measured from the SEM photos). This suggests a large surface tension for condensing drops. Their

faceting occurred either with $[111]$ crystal faces or with numbers of $[110]$ or $[100]$ rough teeth-like edges (**Fig. 2e, f**). In some cases these details were rounded due, more likely, to re-melting the crystallized substance and/or sublimation phenomena that was identified on **Fig. 2g** where several equal in sizes pits were seen to appear on the places found close to inserts' external surface. A case was also observed where a plane was faceting a drop (**Fig. 2e**) that can consider an indication for slower crystal growth on (111) -direction as comparing (100) and (110) directions, owing to mass-redistribution from drop's surface of the observed plane zone to the rest part of the aggregate. In other case there was observed a stem-like single crystal with hexagonal cross-section

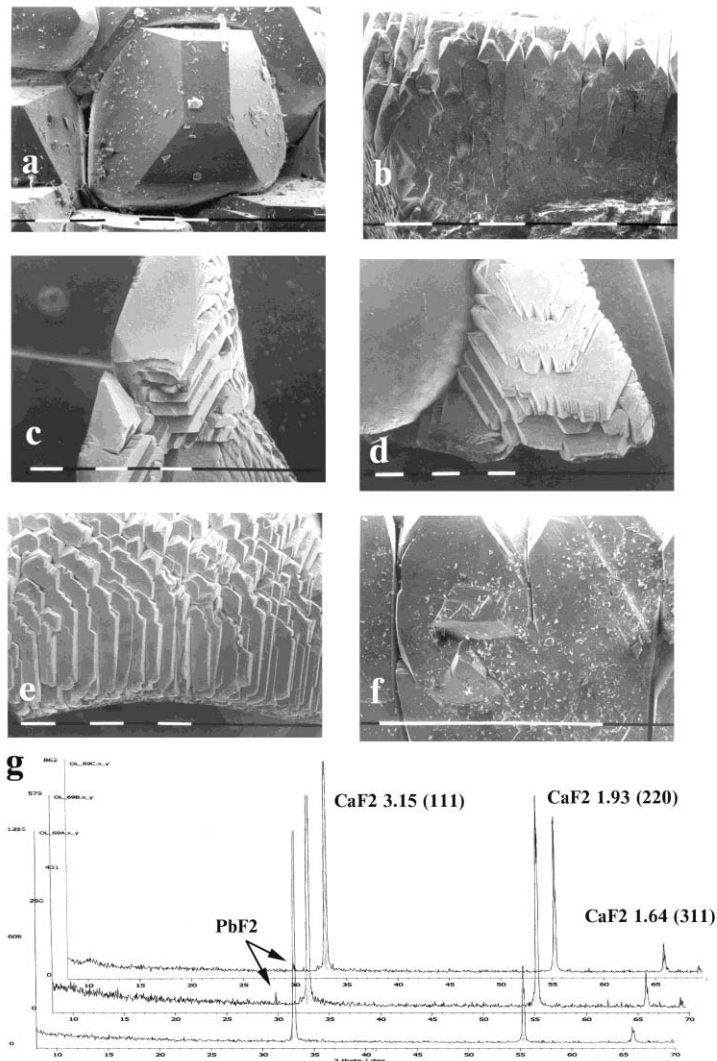


Fig. 3. Longitudinal cross-sectional view in optical microscope of probes taken from the material crystallized in PC: **a**, **b** – stem- and plate-like crystals, crystallized on (100)- and (110)-directions with rectangular and square cross-sections; **c**, **d**, **e** – crystal aggregates – packages of hexagonal plates with acute teeth-like tips; **f** – splitting and secondary selection for growing crystals; **undermost** – X-ray diagrams of three distinguished zones in the grown aggregates.

grown on (111)-direction that was incorporated into a fluorite drop (**Fig. 2h**) where partial re-melting of crystal faces can explain the scale up view of the picture (**Fig. 2k**). At this junction one may suppose the observed hexagonal single crystal has been grown before the condensation and crystallization of the surrounding drop to proceed.

Going further upwards the studied sample aggregate it is seen that from fluorite drops have been grown numbers of equal in sizes and with equal orientation needle- and plate-like crystals. Here some speculative suggestions as regards the nucleation mechanism can be done. In the case under consideration – as contrasted with the crystallization proceeding via (111)-faceting in the condensed drop – the crystallization of the stem- and plate-like crystals was occurred on (100)- and

(110)-directions with clearly seen rectangular and square cross-section (**Fig. 3a, b**).

The orientation of these needle- and plate-like crystals should inherit partially the drop's matrix that bore a specific surface of the aggregates – packages of hexagonal plates with acute teeth-like tips (**Fig 3c, d, e**). It can be supposed a strong competition to proceed between thus growing single crystals in supersaturated by fluorspar vapor ambient. Owing to that, the growth of crystals, being they even insignificantly disoriented outside the general (110) and (100)-directions, would be totally suppressed. Thence specific rounded off cavities arise between the needle- and plate-like single crystals in the region of their expansion. Considerable effect gained as well the structural defects that caused splitting and secondary selection for growing crystals (**Fig. 3f**).

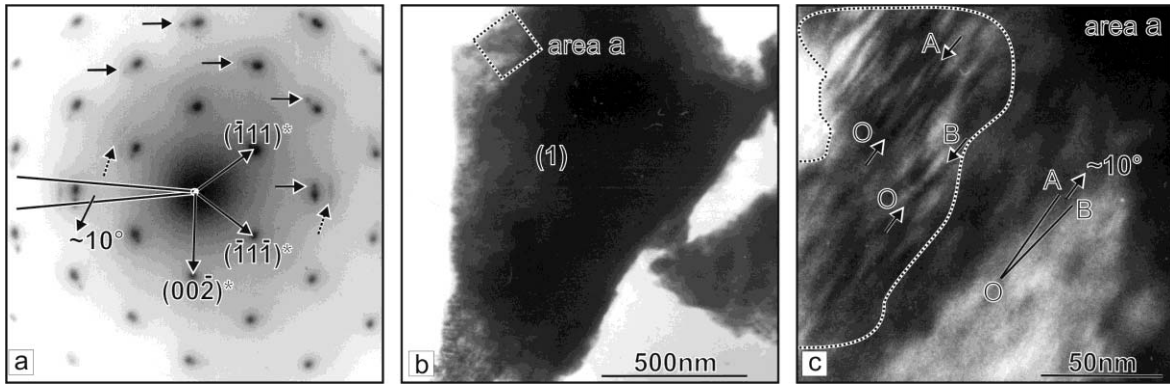


Fig. 4. TEM analysis of probes taken from crystal section shaped during the second stage of growing. **a** – SAEDI along [110] direction of area **a** from crystal (1) shown at (b); **b** – Microcrystal (1) oriented at (110) plane; **c** – above eight as much higher magnification of area **a** from the crystal (1).

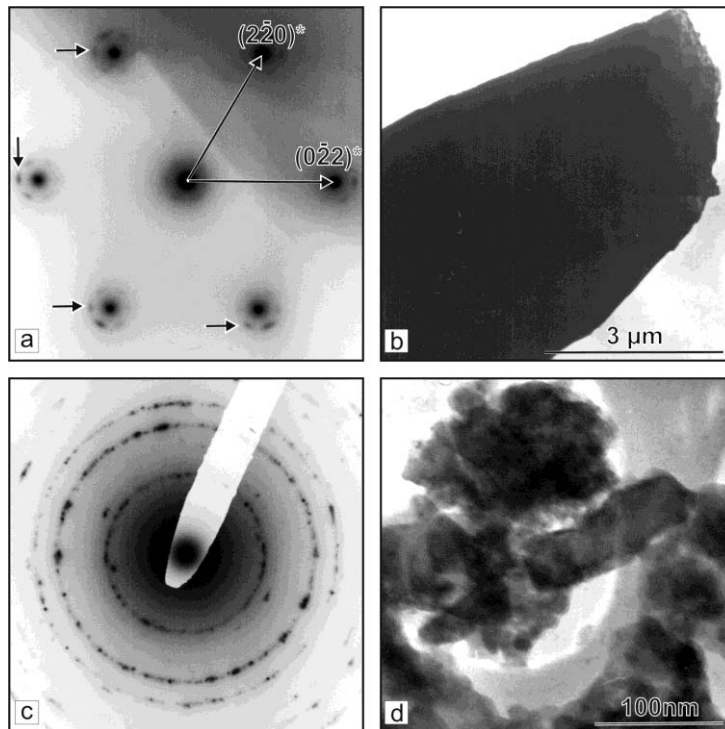


Fig. 5. TEM analysis of probes taken from crystal section grown during the third stage of the process: **a** – SAEDI along [111] direction of round area from crystal shown at (b); **b** – micro-crystal oriented at (111) plane; **c** – polycrystal SAEDI of round area from crystal shown at (d) **d** – microcrystals with grain-shaped structure.

By X-rays phase analysis were distinguished three zones of grown fluorite aggregates, and their stoichiometry were found to correspond of pure CaF_2 without any X-raying peculiarities (**Fig. 3-undermost**).

The electron diffraction analysis performed by TEM manifested the growth of needle- and plate-like crystals on definite fluorite drop should be accompanied by its (111)-epitaxy related to (110)- and (100)-epitaxy for corresponding basic forms. The surface atomic layer should be modulated due to establishing radius for drop's rounding that would cause splitting of the crystal lattice for growing on the drop crystals. These processes were identified on the electron-diffraction pictures as

enlargement and splitting of the index reflection spots.

Three samples thought relevant to different growth stages were investigated by TEM analysis. In the sample corresponding to the *first growth* stage (primary vapour phase crystallization) the μm -sized crystals were observed (**Fig. 4b**). The obtained selected area electron diffraction image (SAEDI) showed that the different particles actually are single-crystals. The point maximums are arc-like splitted and the arcs (indicate with arrow) are curved at round 10° (**Fig. 4a**). After multiple magnifications of the particles (**Fig. 4c**), the diffraction contrast visualized nano-sized defect

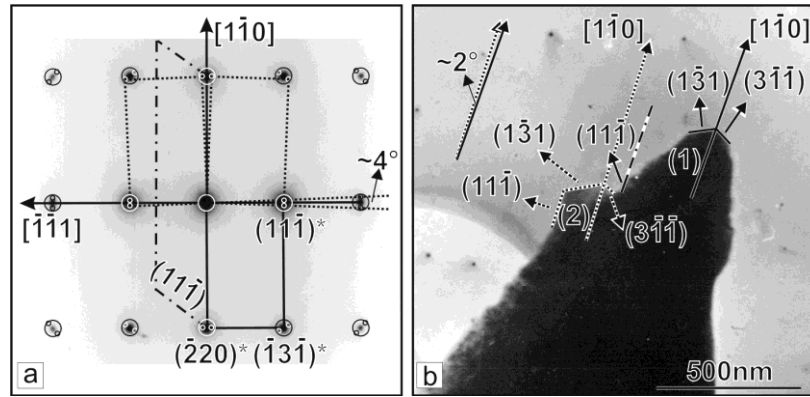


Fig. 6. TEM analysis of probes taken from crystal section grown during the first stage of the process: **a** – SAEDI along [112] direction of area **a** from crystal (1) shown at (b); **b** – micro-crystal (1) oriented at (112) plane.

areas disoriented up to 10°, which coincide with the arc-like splitting of diffraction maximums.

In the sample from the *second growth* stage it was observed a drop-like crystal, round 1 cm in diameter, built from nm to μm separate mono-crystals (**Fig. 5b, d**). SAEDI showed the existence of satellite (indicate with arrow) reflexes, the disposition of which approved a perfect structure of mono-crystals (**Fig. 5a**). The mono-crystals are situated accidentally each by other and formed poly-crystal SAEDI where no proofs for texturization exist (**Fig. 5c, d**).

The sample from the *third growth stage* is present from micro-crystals, grown on the crop-like crystal. **Fig. 6a** shows the SAEDI from [112] direction, resultant from the micro-crystal on **Fig. 6b**.

It is seen that two satellite point maximums are situated at both sides of each main maximum at angle round 2°. The particle morphology shows mono-crystal (marked on **Fig. 6b**. as 1) with [110] growth direction, development of the (131) and (311) crystal faces. One can observe and the second one crystal (marked on **Fig. 6b** as 2 and with dotted lines), fused with the first one on (111) crystal face, and having the same growth direction, development of the same crystal faces. Round 2° fusion angle was measured between the two crystals, which coincides with the angle between the satellite point maximums.

The analyzed view of SEM-microscopy pictures allowed to be reconstructed the growth itself. It was started with slightly disoriented each other nano-crystals joined in micro-crystals, which were differently oriented to the matrix and created a thin layer. After the thin layer was grown the drop-like poly-crystal aggregate was built up from perfect mono-crystals different in sizes. Over them grew up small-angle fused mono-crystals due to the almost spherical matrix. Spectrophotometric analysis (**Fig.**

7) was performed using 4 samples, two of which (sample 1 and 2) were taken from boules grown into different crucible inserts whereas the other two (sample 3 and 4) – from crystallized material after condensation/sublimation of fluorspar vapor in the peripheral crucible compartment during the same growth run. It is seen the spectra of samples 3 and 4, grown from the vapor phase, contain two clear bands which, according to literature [7-10], can be attributed to absorption near 198 and 306 nm due to 4*f* – 5*d* electron transitions in Ce³⁺. The peaks positions for both crystals were found being slightly shifted at 197.3 nm and 302.5 nm, respectively.

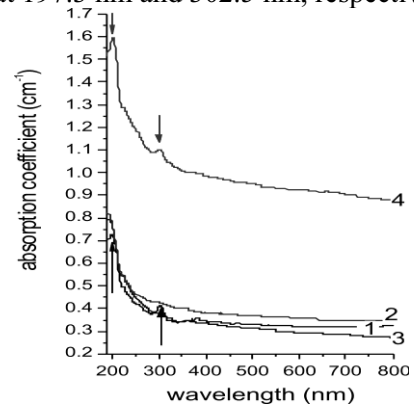


Fig. 7. Optical absorption coefficient spectra of CaF₂ single crystals grown in different crucible compartments from melt (samples 1 and 2) and from vapor phase (samples 3 and 4).

One may suppose that fact is being a result of Sr replacement for Ca into fluorite lattice, the presence of which in the starting raw material was identified by independent AAS analysis to vary within 0.03 and 0.05 wt % [11]. Thence, in accordance with previously published data [12], a conclusion was made the investigated samples can be considered as a mixed Ca_{1-x}Sr_xF₂ system with a very small *x*-proportion where part of Sr bi-valence ions have been replaced by cluster formations of Ce³⁺ ions compensated by F⁻-interstitial. The efficiency of such replacement has been studied being high for

single alkali-earth host crystals [8] as well as for mixed calcium strontium fluoride system [11].

The spectra of samples 1 and 2 (grown from non-vaporized melts in crucible inserts) did not reveal a presence of any absorption bands that suggests, in practice, all Ce ppm-amount has been transmitted from liquid to vapor phase and crystallized thereof aggregates. The absorption coefficient spectra for samples Nos. 1, 2 and 3 are close to each other along the whole visible spectral range, from 400 to 800 nm, manifesting a gradual decrease therein, covered relatively narrow region ($0.4 - 0.3 \text{ cm}^{-1}$). The steeper slope of curve 3, similar to that of curve 4, manifests a better microstructure for both samples grown from vapor phase, despite the curve 4 was located much higher compared to the other three curves, indicating a presence of light-scattering centers, caused by very fine graphite inclusions randomly dispersed in this sample, established by SEM microprobe analysis. At the same time, the performed comparative polarimetry of the investigated four samples showed an absence of residual stresses (deep purple coloration) of samples 3 and 4, in contrast to samples 1 and 2 wherein the deep purple was surrounded by narrow strips of red (22 nm/cm) and blue (108 nm/cm) colors. This result can be explained by external pressure whereupon the growing boules have been undergone from the wall of the inserts while similar effect should not appear in the PC at the places where the crystals were grown free of such pressure. The view and optical properties of crystal aggregates grown in the PC lead to conclusion of their 3-stage formation. Thermodynamically such

suggestion can be supported accepting relevant alteration in P - T conditions according to triple point phase equilibrium: $\text{CaF}_{2\beta\text{cr}} - \text{CaF}_{2\text{melt}} - \text{CaF}_{2\text{vap}}$ established inside the PC. Taking \ln -form for P -phase equilibrium:

$$\ln P(\text{CaF}_{2\beta\text{cr}}) = \ln P(\text{CaF}_{2\text{melt}}) \quad (1)$$

where the vapor pressure – T relationships for tetragonal β - CaF_2 crystal phase and liquid CaF_2 are expressed by [13]:

$$\text{CaF}_{2\beta\text{cr}}: \ln P(\text{atm}) = -53480/T - 0.525 \ln T + 56.08 \quad (2)$$

$$\text{CaF}_{2\text{melt}}: \ln P(\text{atm}) = -50200/T - 4.525 \ln T + 53.96 \quad (3)$$

one can easily calculated the lowest possible t.p. being at $T = 1689 \text{ K}$ ($1416 \text{ }^\circ\text{C}$) and $P = 8.35 \cdot 10^{-5}$ bars or 0.0635 torr. At such P - T conditions established in the peripheral crucible compartment, vapor to crystal phase transition (sublimation) should start on places where $T < 1689 \text{ K}$. At the same time, the maintained low total vapor pressure inside the crucible inserts/central camera provides a mode of bulk boiling into the melts that initiate an intensive vaporization, exceeding considerably the surface evaporation. Besides, the cooling of the lower section of overheated crucible below 1689 K will start in a very short time after it has been moved towards the lower (“cold”) furnace zone.

As higher temperature head has been imposed on fluorspar melts in the inserts, that is, when overheating T has been set up above 1689 K, the sublimation/bulk boiling processes would occur at relevant higher super-saturation pressure $P_{\text{tub}} > 0.0635$ torr following the $P - T$ phase diagram on **Fig. 8a**. Supplement control can be implemented efficiently by appropriate alteration of the effective

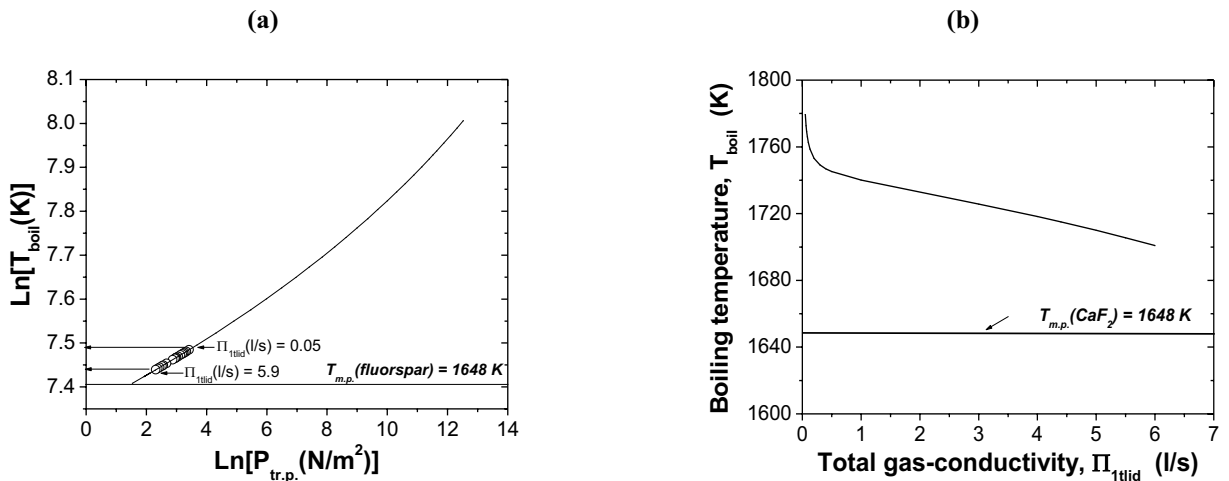


Fig. 8. a – Ln-dependence of boiling temperature on equilibrium pressure inside the different crucible cameras (inserts). **b** – Boiling temperature of CaF_2 melts in crucible inserts versus total gas-conductivity in corresponding lids’ channels.

total gas-conductivity for the system of inner parallel lids' channels and the channel in the general crucible cover (**Fig. 8b**).

For each one P - T combination conditioned being below the equilibrium curve (**Fig. 8a**) the sublimation and bulk boiling will be totally suppressed being replaced by vapor to liquid phase transition (condensation). This will occur when the vacuum system succeeds to maintain a residual pressure inside the crucible below the found lowest value of 0.0635 torr in the t.p. phase diagram. Here the vacuum system influence can be kept under control by altering appropriately the channel gas-permeability of the outer crucible cover so that being provided Knudsen diffusion in it as the slowest possible mass-transport mechanism independent on the mean pressure into the channel. The condensate will start to crystallize upwards on the places, the temperature of which was dropped below the fluorspar m.p. T , that is, near to the bottom of the crucible during its penetration into the cold furnace zone Z2. On this thermodynamic ground, the three stages of aggregates' formation can find a reasonable explanation.

The first stage should cover the initial time interval of crucible movement towards Z2 when P - T conditions in the PC have been adjusted – by appropriate chosen T -pressure and/or channels' gas-conductivities – being stayed higher than P - T phase equilibrium curve shown in **Fig. 8a**. Such thermodynamic conditions mean super-saturation by fluorspar vapor of the free space in this compartment. It occurs when the general channel gas-permeability is being chosen sufficiently low to determined Knudsen diffusion for gaseous/vapor molecules and ions along the channel, whereat its mass-transport resistance restricts the vapor flux towards the vacuum chamber. Such conditions are favorable for appearance of numbers of nucleation centers on definite spots of the inner flatten surface of crucible bottom (bounded by relevant catenaries pertaining to the round solid grounds of the inserts) in conjunction with its microstructure. These centers lead to spontaneous growth of the observed crystallites and very small globules. In fact the established vapor pressure in the compartment depends on both, the effective total gas-conductivity of the system of inner lids' channels and the channel of the general crucible cover. Thus the thermodynamic conditions in the PC may be adjusted precisely choosing appropriate gas-permeability's combinations.

Since the sublimation growth rate upwards is lower as compared to the speed of crucible

withdrawal throughout the adiabatic furnace zone, characterizing itself by a steep negative vertical T -gradient, the mean temperature in the compartment start to decrease, as the T -fall will be faster nearby the sublimating on the ground aggregates. Simultaneously, the level of super-saturation pressure drops down in accordance with strong T -dependence ($\approx T^{2.3}$ [5]) of the attenuating bulk boiling mechanism into the melts. As a result the probability for condensation and following growth of fluorite drops upon the already grown globules/crystallites will rise up sharply (stage 2) what really occurs as it is seen on the pictures in **Fig. 2** and **Fig. 3**.

The last (third) stage supposes the super-saturation to increases again over the equilibrium owing to accelerating growth in the condensed drops whereat the temperature of their tip surface tends to increase rapidly towards the corresponding phase equilibrium value. As a result of that needles and plates start to grow up upon the drops. As intensively these forms are growing as larger the liberated specific heat of crystallization becomes that leads to supplementary re-heating the aggregates with great probability for their partial re-melting. This explains the observed microscopic pictures on **Fig. 2h, k**.

Speculating with these results, one could suppose similar mechanism to induce growth of huge number of various fluorite crystal aggregates at specific Moon's conditions (HV, low gravity, high- T) when, million years ago, large areas of its surface has been occupied by basaltic likes. These likes could think being a source of intensive evaporation of fluorite at low gravity and absence of atmosphere. This mineral may suggest being present in the wombs of the Moon in the very early time of its formation as Earth's satellite. Further, one can suppose the evaporated in the space substance to fall dawn slowly on the surface due to gravity force, whereon to condense and crystallize and/or sublimate on mostly cool poles' regions of the Moon. The very high brightness of 10.0 (and correspondingly estimated albedo) that has been established for certain regions on the Moon (for example the central peaks of Aristarchus [14,15]) means reflectivity close to 100% within a large spectral region. Similar reflectivity spectra are found for investigated CaF_2 aggregates (**Fig. 9**).

As seen the corrected baseline shows 100% relative reflectance, that is, zero absorbance within Vis – near IR. Maximum absorbance is observed in UV region manifested by a slight peak at 265 nm. The similarity for reflectivity spectra pertaining to

aggregates' crystals in study and some Moon's regions is a ground for providing further exploration. This way one could approve or reject the proposed challenging hypothesis for existing nowadays regions on the Moon where to be found any crystalline fluorite.

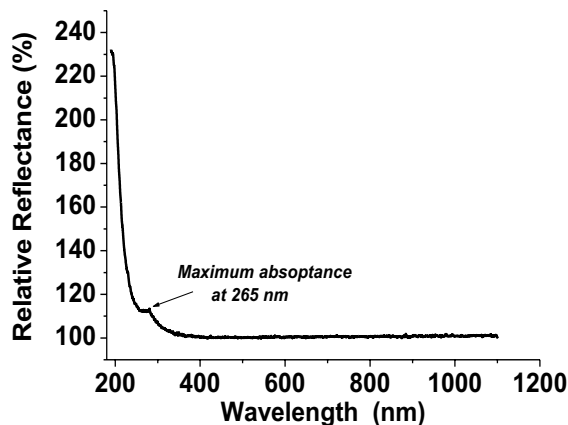


Fig. 9. Reflectance spectrum of CaF_2 powder ground from the aggregates grown in PC of the crucible. The baseline was corrected to spectrum of reference sample: Pretralon – PTFE with reflection of 99% in 400–1400 nm region and >95% – in 200–250 nm region.

CONCLUSIONS

The CaF_2 vapor growth mechanism may be altered controllably to produce complex crystal aggregates depending on established P - T quasi-equilibrium in evacuating permanently space. This is attained by appropriate alteration of temperature head where to are imposed several molten portions of fluorspar in multi-camera crucible accordingly the sizes (gas-permeability) of the channels connecting different section in crucible interior and ambient. Sufficiently small sizes of the channels provide Knudsen type diffusion that determines the slowest possible rate for proceeding mass-transport processes in vapor/gaseous phase that leads to fast super-saturation by CaF_2 vapor the free space in the crucible, the movement of which towards to cooler furnace zone causes relevant alteration in P - T phase equilibrium. The complicated habit of grown aggregates is formed during three consecutively proceeding growing stages in accordance with the induced thermodynamic alterations providing direct vapor to solid phase transformation (sublimation) or indirect one – via vapor condensation and following crystallization. The sublimated crystals appear free of any residual stresses whereas simultaneously grown boules from non-vaporized melts in crucible cameras show stresses' distribution characteristic of the external pressure imposed from cameras' wall on growing crystal. The optical transmission spectrum t of the

boules is considerably better, especially in the UV, comparing to crystal aggregates containing randomly dispersed graphite inclusions, the t -spectra of which aggregates show several peaks of light-absorption specific for calcium strontium solid solution system. The aggregates manifest as well nearly full reflectivity from Vis to near IR region.

The clarification of the growth mechanism of CaF_2 from vapor phase by using natural fluorite as starting material and how it could be efficiently controlled gives opportunity for optimization of the existing but as well for developing new more efficient techniques on the base of effective phase transformation control so that to be produced low cost crystals with improved characteristics at the expense of deep RE-purification of the starting material. These techniques are supposed being appropriate for growing several mixed fluoride crystal systems with unique properties.

The results can be used for modeling fluorite mineralization from vapor phase in HV conditions where the crystal habit is being widely varied. Such models are ground for hypothesizing similar crystals formations could be found on the Moon in differentiated as isolated mineral fluorite deposits.

REFERENCES

1. N.P. Yushkin, N.V. Volkova, G.A. Markova, *Opticheskiy Fluorit*, Nauka, Moskva, 1983, p. 20 (in Russian).
2. J.T. Mouhovski, *Prog. Cryst. Growth Charact. Mater.*, **53**, 79 (2007).
3. K.A. Pandelisev, in: The 2nd Intern Symp on 157 Lithography, Dana Point, CA, USA, 14-17 May 2001.
4. J.T. Mouhovski, V.Tz. Penev, R.B. Kuneva, *Cryst. Res. Technol.*, **31**, No. 6, 727 (1996).
5. I.T. Mouhovski, in: *Optical fluorides: purification and crystal growing, applicability and perspectives*, Akad. Izd. "M. Drinov", Sofia, 2013, p. 145.
6. J.T. Mouhovski, V.B. Genov, L. Pirgov, V.Tz. Penev, *Mater. Res. Innovations*, **3**, 138 (1999).
7. A.A. Kaplyansky, V.N. Medvedev, P.P. Feofilov, *Opt. Spectrosc.*, **14**, 664 (1963) (in Russian).
8. E. Loh, *Phys. Rev.*, **154**, 270 (1967).
9. E. Loh, *Phys. Rev.*, **147**, 332 (1966).
10. D.S. McClure, Ch. Pedrini, *Phys. Rev. B*, **32**, 8465 (1985).
11. I. T. Muhovski, in: *Izrastvane na opticheski kristali ot CaF_2* , NACID, CNTB, Sofia, 2006 (in Bulgarian).
12. B. Kostova, J. Mouhovski, O. Petrov, L. Dimitrov, L. Konstantinov, *Mater. Chem. Phys.*, **113**, 260 (2009).
13. E. Gmelin, in: *Handbuch der anorganischen Chemie*, Weinheim/Bergstr. Verlag Chemie, GMBH., 1976, 8 Auflage, Teil C3, Vol. 39, p. 78.
14. [http://en.wikipedia.org/wiki/Aristarchus_\(crater\)](http://en.wikipedia.org/wiki/Aristarchus_(crater)).
15. <http://www.youtube.com/watch?v=aqpdN5isp8Y>.

ВИСОКОВАКУУМНИ ФАЗОВИ ПРЕВРЪЩАНИЯ НА ФЛУОРИТОВИ ПАРИ В КРИСТАЛНИ АГРЕГАТИ

Й. Муховски*, О. Витов, В. Димов, Б. Костова, С. Гечев

*Институт по минералогия и кристалография "Акад. Иван Костов", Българската академия на науките,
ул. „Акад. Георги Бончев, бл.107, 1113 София, България*

Постъпила на 4 април, 2013 г.; приета на 24 април, 2013 г.

(Резюме)

Комплексни кристални флуоритови агрегати са израсли от парна фаза при специфични $P - T$ условия. Квази-равновесието за протичащите масопреносни процеси, фазовите превръщания и кристално-химичните реакции е постигнато в многокамерен тип тигел чрез промяна на температурния натиск, приложен върху разтопени порции от естествен флуорит и/или чрез подходящо вариране на газопропускливостта на каналите, свързващи различни секции от вътрешността на тигела с околната вакуумна среда. Размерите на каналите са намалени, така че да обезпечат Кнудсенов тип дифузия, ограничавайки по този начин скоростта на паропренасянето през тях, водещо до свръхнасищане на периферното отделение на тигела. Израслите агрегати разкриват сложен хабитус, образуван по време на триетапния процес на израстване и обезпечен от отговорните за това термодинамика и фази. В агрегатите не се наблюдават остатъчни напрежения, докато такива се разграничават ясно в були, едновременно израсли с тях от неизпарената част на стопилките в камерите на тигела. Оптичната пропускливост на булите е значително по-висока от тази, измерена за кристалните агрегати, особено в ултравиолетовия спектрален диапазон, разкривайки няколко ивици на специфична светлинна абсорбция, дължащи се на увеличено присъствие на редкоземни (РЗ) примесни центрове в кристалната решетка. Агрегатите разкриват тяхната практически пълна отражателна способност от видимата до близката инфрачервена спектрални области. Механизмите за растеж от газова фаза при използване на природен флуорит с РЗ примеси са обяснени въз основа на термодинамични съображения, което позволява надежден контрол върху процесите. Предполага се, че резултатите ще спомогнат за разработването на нови перспективни техники на кристален растеж от парна фаза на някои флуорни съединения със сложна структура и състав, но с широко приложение. Може да се допусне, че подобни механизми на растеж на CaF_2 кристали са съществували през началния период от формирането на Луната.